Research article

Role of dolomite as an in-situ CO_2 sorbent and deoxygenation catalyst in fast pyrolysis of beechwood in a bench scale fluidized bed reactor

H. Mysore Prabhakara [*], E.A. Bramer, G. Brem

Thermal Engineering Group, Faculty of Engineering Technology, University of Twente, P.O. Box 217, 7500AE, Enschede, the Netherlands

ABSTRACT

The dual effect of dolomite as a CO_2 sorbent and deoxygenation catalyst in fast pyrolysis of beechwood was investigated. Investigation was performed on a bench scale fluidized bed reactor at an pyrolysis temperature of 500 °C and at different WHSV. CO_2 breakthrough curves and bio-oil samples were produced simultaneously. The results show that dolomite is both a feasible catalyst and a CO_2 sorbent as it produced a moderately deoxygenated bio-oil and a CO_2 free and H_2 rich gas. Acids were eliminated, whereas the concentration of methylated phenols and methylated cyclopentanones were enhanced. These results were achieved when rapid carbonation stage was prevailing throughout the experimental run. An organic rich bio-oil with 9.46 wt% yield and a HHV of 28.0 MJ/kg (as received) was obtained. The pH of the catalytic bio-oil increased from 3.2 to 6.0 and the oxygen content reduced to 21.5 wt% from 47.3 wt%. Moreover, the moderately deoxygenated bio-oil is of interest as it can undergo downstream reforming into wide range of liquid fuels with reduced H_2 consumption. Calculations show that the H_2 generated as a result of CO_2 sorption can suffice the requirement for hydrodeoxygenation. In addition the catalysts were also characterized by BET, XRD and SEM analysis.

1. Introduction

Growing societal concerns regarding climate change, depletion of fossil fuel sources, and fluctuating (uncertain) crude oil prices have resulted in increased interest in bio-based fuels, chemicals, heat and power [1,2]. In this context, lignocellulosic biomass appears to have immense potential as an alternative to fossil fuels for the production of liquid fuels and chemicals [3–5]. In contrast to the first generation of feedstock such as sugarcane and corn, the lignocellulosic biomass utilizes non crop plants and non-edible parts of regular crops to convert them to biofuels. On technological level, fast pyrolysis is regarded to be one of most attractive process for the production of biofuels from lignocellulosic biomass [6–8]. Further, techno-economic analysis has also indicated that fast pyrolysis is economically viable due to its flexibility in feed and products [9]. Fast pyrolysis is a thermo chemical conversion process in which the biomass feedstock is rapidly heated in the absence of oxygen to high temperatures (400–600 °C) with vapor residence time approximatley <2 s at atmospheric pressure. The vapors formed during the process are then condensed to get the liquid product known as pyrolysis oil. Although high yields are obtained, their still exists inherent negative characteristics of the oil such as acidity,

corrosivness, high viscosity and unstable chemical composition which is a result of oxygen containing compounds present in the oil. For example, aldehydes and ketones tend to enhance condensation and polymerization reactions resulting in increased viscosity of the produced oil. Consequently, this limits its direct usage as a transportation fuel or as a feed in the existing petroleum-based refineries [10]. Hence it is essential to remove or modify the oxygen containing compounds to enhance its value.

Accordingly, several methods for deoxygenating the raw pyrolysis oil have been proposed to facilitate its valorization into fuels and/or raw chemicals. For instance, considerable amount of research has been done on catalytic processes such as hydrodeoxygenation (HDO), catalytic cracking, esterification and reactive distillation [11]. However commercial implementation is far from reality due to problems such as the repolymerisation of the bio-oil, catalyst deactivation, reactor clogging and high hydrogen consumption. On the other hand, in-situ catalytic fast pyrolysis has received increased attention in promoting deoxygenation reactions to convert biomass into a liquid product containing mixture of aromatics and olefins [12–15]. Further, its potential to be integrated into mainstream refinery infrastructure seems to be economically beneficial [16]. In this process, the pyrolyis vapors come in contact with

the catalyst as they are produced before it condenses. This method has an advantage of preventing some of the repolymerization and gum forming reactions that occur in liquid phase deoxygenation process.

Zeolite Y, Beta, Mordenite, ZSM-5, MCM-41, FCC, hierarchical zeolites, metal modified zeolites and HZSM-5 are among the most widely evaluated in-situ catalysts for the pyrolysis vapor upgrading [17–20]. Among these zeolites, HZSM-5 has shown promising results in lowering the content of oxygenates and producing the desired aromatic hydrocarbons in pyrolysis bio-oil. This effect has been mainly attributed to shape selectivity, unique three-dimensional microporous structure and density of acid sites on the catalyst [21–23]. In the presence of zeolite catalyst, the pyrolysis vapors diffuse into the pore channels of the zeolite and undergo a variety of reactions at the Brønsted and Lewis acid sites to form olefins and aromatics via hydrocarbon pool mechanism [24,25]. However these catalysts primarily favour oxyen removal in the form of H_2O and CO which is less energy optimal compared to oxygen removal as CO_2. Moreover, high rate of coking and physically deterioration (attrition, sintering and/or agglomeration) over repeated cycles have been has been observed in a recent pilot scale study [26]. All these factors increase the catalyst deactivation rate, and hence the economics and sustainability of the process are negatively influenced.

Considering the limitations of solid acid catalysts, nature-derived calcium based minerals have gained increased interest as an alternative [27]. These minerals can be generally procured at relatively lower price and their un-calcined precursors are abundantly available. Among them, dolomite ($CaMg(CO_3)_2$) has been frequently cited as a catalyst to reduce tars in biomass gasified syngas [28–30]. For example, Berrueco et al., [30] used dolomite to decrease the tar yield by 51% during gasification of Norwegian spruce at 750 °C. Tar removal capability of dolomite is mainly ascribed to both steam and dry reforming reactions which are active in the calcined form (CaO–MgO) [31,32]. Besides tar reforming ability, calcined dolomite can react with CO_2 to form carbonates depending on the process conditions. For example, Johnsen et al. [33] applied dolomite as a CO_2 sorbent to shift the equilibrium of water gas shift reaction during steam reforming process of natural gas. As a result, the product gas consisted of 98% H_2-concentration on a dry basis at 600 °C and 1.013×10^5 Pa.

Additionally, dolomite has also been investigated in the context of in-situ biomass pyrolysis which is relevant to the present investigation. For example, both oxygen content and acidity of the bio-oil decreased when dolomite was used in an auger reactor and fluidized bed reactor respectively [34,35]. Further, increment in hydrogen (H_2) concentration was observed primarily due to the ability of dolomite to continously remove CO_2 from the pyrolysis vapors and drive the equilibrium-limited water gas shift (WGS) reaction towards internal production of H_2. Nevertheless, the pyrolysis gas still contained 38.7% and 24.7% CO_2 respectively on N_2 free basis and the bio-oil still consisted of undesiable components such as acids, carbonyls and phenols. Similarly, sugar cane straw was pyrolyzed in the presence of dolomite yielding a bio-oil with a lower oxygen content but no details about the gas concentrations were provided [36].

Summarizing, at this point it should be noted that only limited studies exist where dolomite has been investigated as an in-situ catalyst for reforming biomass fast pyrolysis vapors. Moreover, the extent of deoxygenation possible and possibility of obtaining a pyrolysis gas completley free of CO_2 and rich in H_2 is not known form the literature. Hence it opens up a possiblity to explore the ability of dolomite to simultaneousy deoxygenate pyrolysis vapors and to produce a gas completley free of CO_2. It is also important to quantify if the increment in hydrogen can suffice the requirment of downstream process such as hydrodeoxygenation (HDO). Therefore, this present research aims at unravelling the dual functionality of dolomite in CO_2 sorption and deoxygenation in catalytic in-situ upgrading of pyrolysis vapors. A bench scale fluidized bed reactor was operated with continuous biomass feeding to simultaneously generate CO_2 breakthrough curves, corresponding H_2 curves and bio-oil samples to understand the potential of

dolomite in pyrolysis of biomass. Additionally dolomite before and after pyrolysis of biomass were characterized by BET, XRD and TGA.

2. Materials and methods

2.1. Biomass

Wood fibres by the commercially name Lignocel by J. Rettenmaier & Söhne GmbH were used as the biomass for the experiments. Particle size was in the range of 0.15 to 0.5 mm. The samples were dried at 105 °C for 24 h and then stored in an air tight container. Table 1 shows the condensed ultimate and proximate analysis of the dried beech wood. Elemental analysis of beechwood was done according to ASTM D5291–16 by using an Inter-science Flash 2000 elemental analyser. Mass fraction of oxygen was calculated by difference. Sulphur content was not measured in the setup used and was considered negligible. Typically beechwood contains around 0.02 wt% sulphur and thus it can considered negligible although it affects the accuracy of oxygen content [37]. The proximate analysis was conducted on a TA instruments Q5500 TGA under nitrogen flow and in the temperature range of 30–950 °C with the heating rate of 10 °C/min.

2.2. Dolomite preparation and characterization

Dolomite with the trade name MICRODOL® 1 was procured from OMYA. The received dolomite particles were sieved to particle sizes 300 to 400 μm and then calcined in air for 4 h. at 800 °C so that the calcium magnesium carbonate was thermally decomposed into the CaO and MgO. Thermogravimetric analysis (TGA) was performed on a Q5500 TGA to determine the thermal decomposition characteristics of dolomite. The analysis was made in a flowing air atmosphere in the temperature range of 30–900 °C with a heating and cooling rate of 10 °C/min.

X-Ray diffractometer (XRD) analysis was done on a Bruker D2 Phaser XRD device using a Cu Kα1 radiation source (40 kV, 40 mA). Diffractograms were recorded over the range 2θ = 10–80°, scanning rate of 1°/min and with a step size of 0.05°. Surface characteristics of the catalysts were measured using N_2 adsorption-desorption isotherms at 77 K by employing a ASAP 2400 micromeritics equipment. The surface area was calculated by the application of the BET equation; the surface area of the micropores was obtained by applying the t-plot method; BJH calculations were applied for obtaining pore size distribution and average pore diameter. The morphology of fresh and spent dolomite was studied on a JEOL model JSM-6490LV scanning electron microscope (SEM).
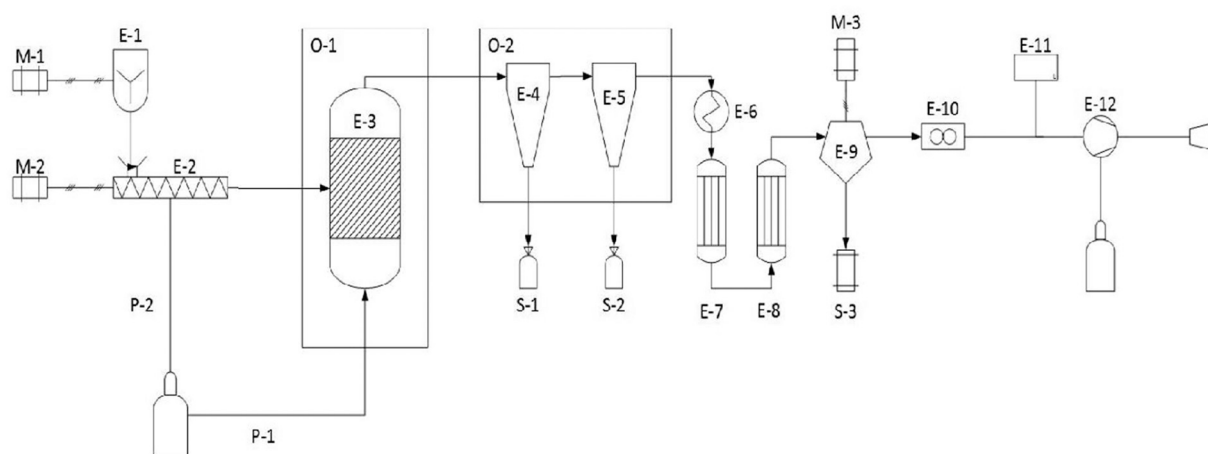
2.3. Fluidized bed reactor

The experimental campaign was performed with a bench scale bubbling fluidized bed. Fig. 1 depicts a schematic of the experimental setup. The setup is located in the Klein horst laboratory of the University of Twente. The experimental system mainly consisted of five section namely, a feeding system, the bubbling fluidized bed reactor, solid separator (cyclones), cooling/condensation system and the gas analysis equipment.

The feeding system consisted of a biomass hopper which fed the biomass on to a fast running screw which conveyed the biomass into the

Table 1

Ultimate and proximate analysis of dry biomass.

Ultimate Analysis (Wt% dry basis)				Proximate Analysis (Wt% dry basis)			
C	H	N	O[a]	Moisture	Volatiles	Fixed Carbon	Ash
48.7	6.1	0.1	45.1	–	84.87	14.53	0.59

[a] By difference.

No.	Description
P-1	Nitrogen (Fluidizing gas) line to the reactor
P-2	Nitrogen line to the feeding section
E-1	Feeder
E-2	Fast Running Screw
E-3	Fluidized Bed Reactor
E-4	Big Cyclone
E-5	Small Cyclone
E-6	Condenser
E-7	First Heat Exchanger
E-8	Second Heat Exchanger
E-9	Rotational Particle Separator
E-10	Flow Meter
E-11	Gas Analysers
E-12	Venturi
M-1	Feeder motor
M-2	Fast Running screw motor
M-3	RPS motor
S-1	First Char storage
S-2	Second Char storage
S-3	Bio-oil storage
O-1	Reactor ovens
O-2	Cyclone ovens

Fig. 1. Bench scale fluidzied bed reactor setup for biomass pyrolysis.

bubbling bed consisting of sand and/or dolomite. The hopper feeder was regulated by a frequency regulator (SLM 2200–1) electrical motor and the fast running screw was powered by an electrical motor that runs at a constant speed. The inlet of the fast screw to the fluidized bed was located 5.5 cm above the distributor plate. Nitrogen was supplied to the fast running screw to prevent back flow during the experiment. Cooling air was provided along the outside periphery of the fast screw to prevent any initiation of pyrolysis of biomass in the feeding section.

The reactor was fabricated from a stainless steel and it had a diameter of 84 mm and a wall thickness of 2 mm. The reactor has a total height of 65 cm, including a 25 cm pre-heating zone below the gas distribution plate. The bottom of the pre-heater was designed as an inward cone to improve the flow distribution and was also filled with large steel particles to enhance the heat transfer rate to the fluidizing gas. Nitrogen was used as the fluidizing gas and it was introduced into the reactor via a distribution plate made out of a 10 mm thick compressed glass fiber. Silica sand and/or dolomite with particle size of 300– 400 μm was used as the fluidized bed material. The static bed height was 15 cm and the freeboard was 28 cm long.

The fluidized bed reactor was placed inside two vertically stacked electrical ovens. The temperatures of all ovens in the setup were measured and controlled by the relay cabinet and a Windmill Microlink 752 RTD system. The actual temperatures were measured by the K-type thermocouples placed inside the ovens. Two additional thermocouples were located inside the reactor which recorded the bed temperature and the temperature in the splash zone just above the bed. The pressure in the reactor was measured with two pressure gauges located at the

entrances of the preheater and at the top of the freeboard respectively. Further, the tubes connecting the reactor to cyclone and condensers were maintained at 500 °C in separate ovens to avoid the condensation of pyrolysis vapor inside the tubes. The solid particles entrained from the fluidized bed were separated by two cyclones in series. These two cyclones are able to collect all char particles greater than 22 μm with an efficiency of 99.9%. At the beginning of each experiment, the bed material was weighed and then placed into the reactor. After the experimental run, both char and bed material were collected from the cyclone and the reactor respectively.

The cooling system consisted out of a pre-cooler in series with a shell and tube heat exchanger. They were maintained at a temperature below -5 °C using a circulator with a mixture of ethylene glycol and water as the cooling solvent. Further downstream, a rotating particle separator (RPS) filtered out any solids, mists and aerosols from the non-condensable gasses using a rotating filter. The RPS can very efficiently capture the mist of oil vapors and almost a vapor free gas leaves the RPS. Finally it was possible to collect all the condensed liquid from the reservoir attached to the RPS at the end of the test run. A venturi is placed after the flow meter to regulate the pressure in the set-up.

The outlet temperature of the gas was measured by a thermocouple connected at the exit of the RPS. Further, the volume flow of the gases passing through the system were measured using an Itron G4 gas flow meter with an accuracy of 0.2 L (<1% error) which was installed after the RPS. Due to its accuracy, comparing the flows at the inlet of the system and at the end gives a good indication of mass balance closure of the setup. A sample of this stream was then pumped to an on-line gas

analysis unit consisting of gas conditioning system with its outlet connected to an gas analyzers. The infrared gas analyser was used to measure the CO_2 concentration and the micro gas chromatograph was used to measure the CO, H_2, CH_4 and O_2 concentrations. The ideal gas law calculations were employed to estimate the molar amount of each gas and close the mass balance.

2.4. Experimental conditions

The pyrolysis experiments were carried out at 500 °C. The biomass feeding rate was 0.5 kg/ h. The gas velocity was controlled to maintain a vapor residence time in the reactor less than 2 s and to assure a adequate mixing of the fluidized bed. The gas velocity was approximately thrice the minimum velocity. The operating parameters are listed in Table 2

2.5. Product analysis

Elemental composition of bio-oil was done according to ASTM D5291–16 by using an a Flash 2000 (Interscience) instrument. In this analysis, the samples were completely oxidized in oxygen and the carbon, hydrogen mass fractions were calculated directly based on the amount of CO_2 and H_2O formed, and the oxygen mass fraction was obtained by difference. The water content of bio-oil was determined using Karl Fischer titration (using Metrohm 787KF titrator). The higher heating value of bio-oil was determined by a bomb calorimeter unit (IKA C2000). The pH of the pyrolysis oil was measured with a Thomas Scientific 675 pH/ISE meter at ambient temperature conditions.

Agilent GC–MS (7890A- 5975C) with a HP-5MS capillary column (30 m × 0.25 mm × 0.25 μm) and helium as a carrier gas (flow rate of 2 mL/min) was used to analyze the composition of bio-oil. GC–MS was also equipped with a flame ionization detector (FID). The column temperature was maintained at 45 °C for 4 min, increased to 280 °C at a heating rate of 3 °C/min and then maintained for 20 min. The identification of the peaks was accomplished by matching the mass spectra. The NIST 2.0 library is used to detect the components. Physicochemical properties and chemical compositions were determined for each phase in the case of visible phase separation.

3. Results

3.1. Non-catalytic pyrolysis

Initially, a set of trial experiments were conducted on the bench scale fluidized bed reactor to optimize the pyrolysis reaction conditions. The aim was to obtain the product distribution and physio chemical parameters of the products and compare them to those reported in the literature. A good result was achieved by continuously operating the setup for 60 mins at a pyrolysis temperature of 500 °C, fluidization velocity of 0.18 m/s and a biomass feed rate of 0.5 kg/h. Other relevant operating conditions are shown in Table 2. Subsequently this set of parameters were used as reference to compare the effect of dolomite on

Table 2
Fluidized bed operating conditions.

Operating Conditions	Value
Reactor Temperature (°C)	500
Biomass Feed rate (kg/h.)	0.5
Fluidizing gas (N_2) Flowrate (l/min)	25
Min. fluidization velocity sand (m/s)	0.07
Min. fluidization velocity calcined dolomite (m/s)	0.04
Fluidizing gas (N_2) Velocity (m/s)	0.18
Vapor residence time in Reactor (s)	1.8
Coolant Temperature (°C)	−5
Cyclone Oven Temperature (°C)	500
Bed Material mass (kg)	1
Experimental Time (Mins.)	60 & 30
Dolomite loading (WHSV) (hr^{-1})	5, 2.5, 1.6, 1.2 & 0.8

the product distribution, CO_2 capture and deoxygenation ability. The results from this experiment are from now denoted by the non- catalytic experiment.

The product yields for the optimized non- catalytic experiment on the basis of total mass of biomass fed into the system were 61.1% bio-oil, 15.1% gas and 12.8% char which added up to 89.0% mass balance closure. The non-catalytic bio-oil consisted of 48.8 wt% of organic fraction and 12.3 wt% yield of water. In practice these two phases cannot be readily separated and are therefore often considered as one phase. Similar results were obtained when beechwood was pyrolyzed in a fluidized bed reactor [38–40]. For example, investigation by Wang et al. [39] resulted in 65% bio-oil, 17.7% gas and 15.9% char on biomass feed basis.

The major components in the pyrolysis gas were CO and CO_2 with yields of 8.0 and 6.1 wt% respectively. Hydrogen and methane only accounted for a very minor portion of the gas with 0.04 and 0.9 wt% respectively. The concentration of these gases corrected for N_2 dilution in the effluent gas stream with respect to experimental run time is plotted and shown in Fig. 2. The gas concentrations tend to reach dynamic equilibrium within a short span and time and thus confirming the uniformity of the process. This is a very important indicator showing that the overall process was stable and reliable. Moreover, the temperature was more or less constant and was within 2–3 °C for the entire experimental run. The temperature profile in the fluidized bed over an experimental time of 60 min is shown in Fig. 2 (b). Hence this indicates that there were no heat transfer limitations for a uniform pyrolytic decomposition of biomass to happen within the bed. This is also confirmed the uniformity of the bubbling fluidized bed. This forms the
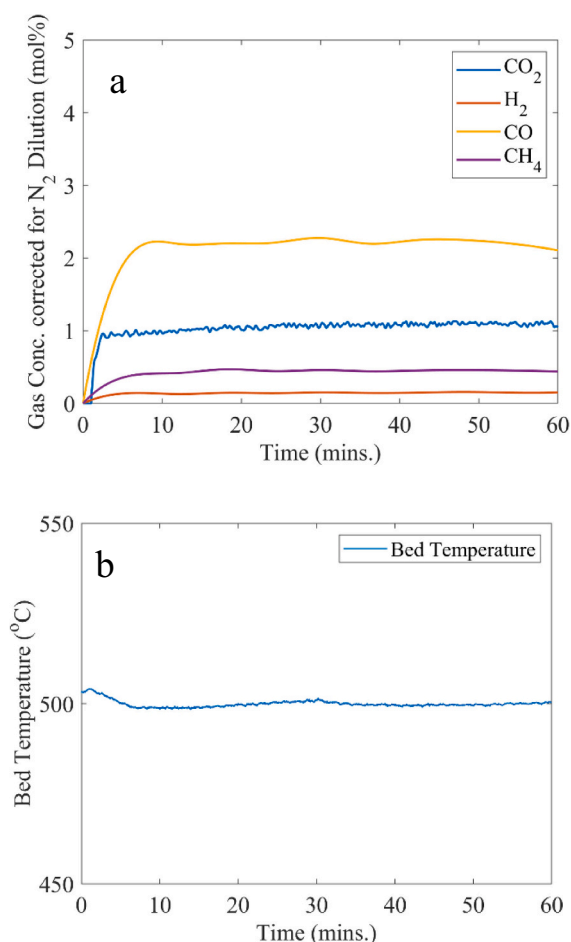
Fig. 2. (a) Major Gas concentration profiles (corrected for N_2 dilution) during non catalytic pyrolysis (b) Temperature profile- non catalytic pyrolysis.

basis for comparing possible changes in gas concentrations during catalytic pyrolysis using dolomite.

The Physio-chemical properties of the bio-oil in comparison with heavy fuel oil are shown in Table 3. Heavy fuel oil is an example for a fuel which finds applications in variety of areas such as district heating and shipping vessels. Recent concerns over its environmental implications have prompted interests in alternatives such as biomass pyrolysis oil. The higher heating value and pH of bio-oil was found to be 18.12 MJ/Kg and 3.23 respectively. This is a direct impact of the high oxygen content in the bio-oil. In contrast to bio-oil, heavy fuel oil has a substantial 85.30% carbon and 11.47% hydrogen content respectively resulting in a product with a higher energy content. Further, to discern the chemical composition of the bio-oil, a GC–MS technique was employed. The detected chemicals were mainly categorized into 8 groups based on their oxygen functionalities. These groups are namely acids, aldehydes, ketones, anhydro-sugars, furans, phenols, hydrocarbons. Small, unidentifiable peaks were grouped together as others. The relative TIC area % of each group was estimated as the sum of areas of all detected peaks in that group divided by the total peak area of all the compounds detected. Fig. 3 shows the relative proportions of different groups in the bio-oil. This method yields semi quantitative results and it has been commonly used by other authors [41,42]. It is a useful tool to differentiate between the concentrations of components in bio-oil obtained under different conditions. The GC–MS analysis of thermal pyrolysis bio-oil revealed that the phenols were the most abundant group (25.9%) followed by acids (22.7%), aldehydes (13.1%) and anhydro-sugars (11.1%). Further, furans and ketones were also present in relatively smaller amounts. More specifically the bio-oil consisted of a mixture of multifunctional oxygenates such as acetic acid, 1,6-Anhydro-β-D-mannopyranose, 2-Propanone-1-hydroxy, furfural, 3-ethyl-2-hydroxy- Phenol and 2-methoxy-4-(1-propenyl)-,(*E*)- etc. These compounds are undesirable as they downgrade the physiochemical properties of the bio-oil. For example, the presence of acids in pyrolysis oil is known to negatively affect its properties and moreover problems may occur during utilization in combustion engines owing to corrosion. In general the aim of the catalyst is to remove these oxygenates and preferably convert them into hydrocarbons to improve the bio-oil in terms of heating value and other physio-chemical parameters to meet the requirements of end use. Results of catalytic pyrolysis are discussed next.

3.2. Catalytic experiments- effect of WHSV (dolomite loading)

In this section the influence of dolomite on the in-situ deoxygenation and in situ CO_2 capture are discussed. The overall aim of these experiments was to investigate the possibility of simultaneously improving bio-oil characteristics and to produce a gas rich in H_2. In order to achieve this, series of continuous experiments were conducted at pyrolysis temperature of 500 °C, 0.5 kg hr^{-1} biomass flowrate and varying the weight hourly space velocity (WHSV). WHSV was varied by replacing part of the quartz sand (bed material) with dolomite on mass basis. WHSV is defined as the ratio of biomass flow rate to the mass of dolomite in the bed. The mass of the total bed material remained the same for all the experiments. The other relevant parameters remained the same as in

Table 3
Physio-chemical properties of non catalytic bio-oil in comparion to fuel oil (as received).

	Thermal	Heavy Fuel Oil[10]
Water (%)	20.1	0.1
C (Wt%)	45.7	85.3
H (Wt%)	7.3	11.4
N (Wt%)	0.6	0.3
O^a (Wt%)	46.3	1.0
pH	3.2	5.7
HHV	18.1	40
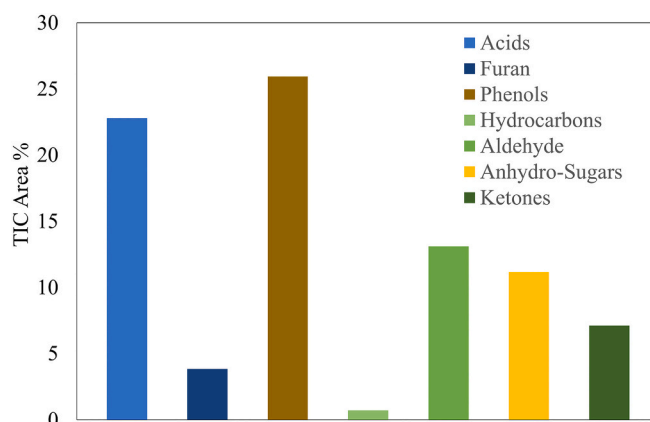
Fig. 3. Chemical composition on non-catalytic.

the optimized thermal pyrolysis experiment. In total 5 experiments were conducted with WHSV ranging from 5 to 0.83. As a result of these experiments, CO_2 breakthrough profiles were generated along with production of bio-oil. In the following subsections, initially the mass balance is discussed, followed by the impact of dolomite on the gas production and finally the characteristics of the bio-oil are discussed. The experimental time was 60 mins for all the experiments discussed in this section. Following these experiments, an additional experiment was carried out at WHSV 1.25 and an experimental time of 30 mins. It is denoted as 1.25$^{\#}$ to differentiate between the experiment conducted for 60 min at WHSV 1.25.

3.2.1. Mass balance

The yields of bio-oil, char, heterogenous char (h-char) and gas based on the total biomass fed is shown in Table 4. In this case, h-char is a result of CO_2 captured and coke deposited on the dolomite during pyrolysis. Mass of h-char was measured by taking the difference between mass of the bed material before and after the experiment. The h-char increased with an increase in dolomite loading. This is a direct result of enhanced in-situ CO_2 being captured and coke deposition. The amount of CO_2 captured is quantified and discussed in a later section. On the contrary, the yield of char did not show a major change and remained more or less the same with increased dolomite loading. This is very likely as the average amount of biomass fed to the reactor during each of these runs were same (0.5 ± 0.01 kg/h.). As the dolomite loading increased the bio-oil yield drastically reduced. The total bio oil yield reduced from 61.1 wt% to a range between 48.4 wt% and 20.0 wt% depending on the WHSV. On the contrary, when a mixture of sand and dolomite was used in a auger reactor the bio-oil yield only reduced up to 2% [34]. This can be explained by the fundamental differences in reactor setup. In our case, the fluidized bed allowed for uniform mixing of the sand and dolomite and thus the gas to solid interactions were enhanced leading to reduced yields and higher CO_2 capture. This also meant that the potential to deoxygenate the pyrolysis vapors were also enhanced. Other investigations of catalytic fast pyrolysis on fluidized bed reactor reported the optimum yield of bio-oil in the range of 29– 50 wt% [43–47]. For example, the application of zeolite HZSM-5 and redmud reduced the bio-oil yield from 60.1 wt% to 49.34 and 44.37 wt% respectively [45]. Further, the yield of gas was slightly reduced as a result of CO_2 capture and with increasing dolomite loading a gas sparse in CO_2 and rich in H_2 was generated as shown in Table 4. In the following section, the gas products are discussed in detail.

3.2.2. Gas analysis

In Fig. 4 (a), the volume fraction of CO_2 measured in the effluent gas as a function of time are plotted for different WHSV. As a consequence of the sorption ability of dolomite, CO_2 was not detected in the effluent gas upto a certain experimental time. After a certain time, the CO_2

Table 4
Mass balance based on total biomass fed- effect of dolomite.

	Product	Non-catalytic	WHSV 5	WHSV 2.5	WHSV 1.66	WHSV 1.25	WHSV 0.83	WHSV 1.25$^{\#}$
Dolomite conc. in bed (%)		0	10%	20%	30%	40%	60%	40%
Run Time (Mins.)		60	60	60	60	60	60	30
Product Yield (Wt%), Total biomass fed basis	Gas	15.1	14.2	12.9	12.6	11.3	11.4	10.8
	Char	12.8	8.5	9.0	11.3	9.4	12.4	10.7
	Heterogenous Char	–	15.7	23.7	30.2	36.8	45.7	38.1
	Total Bio-oil	61.1	48.4	40.4	31.5	27.8	20.0	25.2
	Total Water	12.3	11.5	14.4	17.6	15.6	11.4	15.1
	Total Organics	48.8	36.9	25.9	13.9	12.2	8.6	10.1
	Mass Closure	89.0	86.8	86.1	85.7	85.4	89.6	87.8
Gas (Wt%)	CO_2	6.1	4.7	2.8	1.6	0.5	0.12	0
	CO	8.0	7.9	7.7	7.6	7.0	6.9	7.0
	H_2	0.04	0.16	0.38	0.65	0.74	1.04	0.68
	CH4	0.9	1.3	1.9	2.6	2.9	3.2	3.1
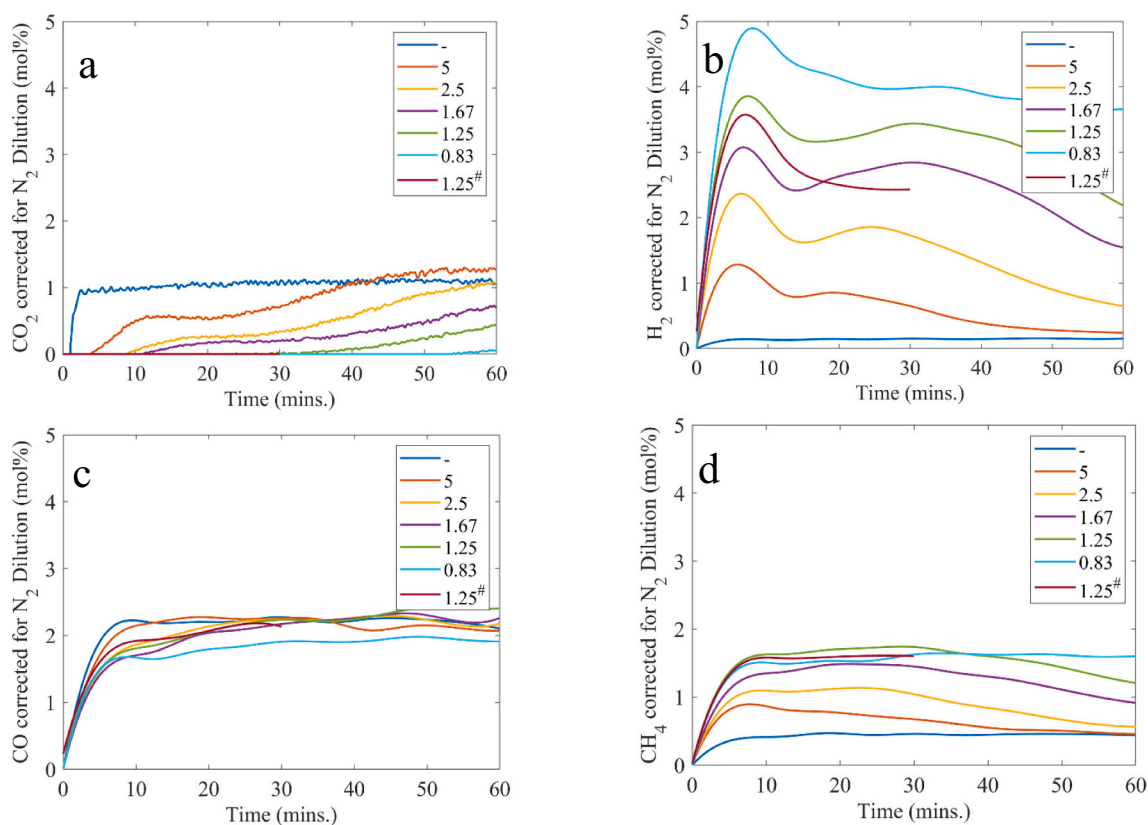
Fig. 4. Gas concentrations (corrected for N2 dilution) due to different WHSV (dolomite loading) (a) CO_2 (b) H_2 (c) CO (d) CH4.

concentration in the effluent gas increased and this rapid change is termed as "breakthrough". The breakthrough times increased from 4 min up to 54 min as the dolomite loading increased. Following the breakthrough, the effluent CO_2 volume fraction increased steadily over the streaming time of 60 mins. There seems to be no dynamic equilibrium established except for WHSV 5 indicating that the dolomite continued to take up CO_2 at a lower rate than at the rate before breakthrough.

The CO_2 capture process using calcium based sorbents is a multi-faceted heterogeneous reaction. In this study, two distinct stages can be observed from the CO_2 breakthrough curves Fig. 4 (a). Firstly, a very rapid carbonation stage up to a breakthrough point was observed and secondly a sluggish stage evolved post the breakthrough point. The chemical reaction kinetics of the reaction CO_2 with CaO dictates the rapid carbonation stage. The sluggish stage is due to the plugging of the pores by dense $CaCO_3$ product layer around the unreacted CaO. It means

that the diffusion through the dense $CaCO_3$ product layer was limited and it determined the new reaction rate of carbonation. The onset of this slow stage accompanied by loss in surface area which limits the practical sorption capacity of dolomite. Such analysis is supported by several studies where the gas-solid CO_2-CaO reaction occurs via two consecutive rate controlling regimes [48–50]. At this stage, it should be noted that it is not feasible thermodynamically for the MgO component of dolomite to capture CO_2 and hence the discussion is mainly on the CaO. Further, depending on the temperature and CO_2 partial pressure there can also be an initial induction period apart from the rapid and slow carbonation stages discussed above. However such an induction period was not observed in the experiments conducted in this study. It is generally observed on an experimental setup such as a thermogravimetric analyser (TGA), where there are mass transfer limitations.

As a consequence of CO_2 sorption, the equilibrium of the water gas shift reaction was shifted towards hydrogen production. It is evident

from Fig. 4 (b) where volume fraction of hydrogen as a function of time is depicted for varying WHSV. The concentration of H_2 rapidly increases and it reaches a peak value before dropping and stabilizing for a brief period and eventually dropping off steadily. The initial spike and drop in the initial spike and the subsequent stabilization are also correlated with the bed temperature profile as shown in Fig. 5. The bed temperature profile was recorded by the thermocouple located in the center of the dense section of the bed with respect to experimental time. As the exothermic CO_2 sorption reaction is initiated, the bed temperature reaches a peak value and gradually drops and stabilizes as the hotter bed gets mixed in the course of the experiment. Further at the end of the fast carbonation period, the temperature and also the hydrogen concentration steadily decrease. Moreover, as the bed temperature spikes during the initiation of the fast carbonation it results in enhanced degradation of the lignin component in the biomass resulting in additional hydrogen production apart from the hydrogen from equilibrium shift in the WGS reaction. In general, the stabilized temperature region corresponds to the fast sorption stage and the temperature reduction corresponds on the onset of the sluggish carbonation stage. Overall, the H_2 concentration increased with the dolomite loading as more CO_2 was captured. It was expected that the temperature spike will also increase in accordance with the H_2 spike with increasing dolomite loading. However that was not the case, especially as the dolomite concentration in the bed was increased to 60% (WHSV 0.83). It is possible that the fluidization characteristics (mixing behavior), average specific heat, particle to particle heat transfer and the ongoing deoxygenation reactions were altered slightly as the dolomite loading increased to 60% in the bed. Therefore it can inferred that the H_2 spike in the case of 0.83 is predominantly due to CO_2 sorption. It can also be observed that the H_2 concentrations for the experiments conducted at WHSV 1.25 and WHSV 1.25[#] showed a slight variation and this can be explained by the approximate 3– 5 °C difference in the temperature spike recorded in the bed.

In addition, methane concentrations increased as the dolomite loading was increased. This can be attributed to the breakdown of the lignin derived aromatics catalysed by dolomite. Such observations were made when aromatics were pyrolyzed in the presence of CaO [51]. Overall the concentration profile of CH_4 showed an initial raise and gradually decline over the run time as the fast carbonation period elapsed Fig. 4 (c). As a general sense it was expected that the CO concentrations will rapidly decrease in order to balance the water increase via dehydration reactions and CO_2 depletion via sorption. However, CO concentrations decreased to a limited extent and it was at its the lowest value when dolomite loading was at maximum. Probably there must have been promotion of decarbonylation reaction during biomass

pyrolysis leading to the formation of additional CO. Moreover, equilibrium calcuations are required to estimate the extent to which CO conversion is possible. However this was out of the scope of this research. Overall concentrations of CO tended to stabilize just below the thermal pyrolysis concentrations as shown in Fig. 4 (d). Further, the bio-oil characteristics are discussed.

3.2.3. Physio chemical properties of bio-oil

Physio-chemical properties of both non-catalytic and catalytic bio-oils are tabulated in Table 5. In each case, bio-oil was collected at the end of 60 mins except for the experimental run at WHSV 1.25[#]. The higher heating value (HHV) of the non-catalytic bio-oil was found to be 18.1 MJ/Kg with a pH of 3.0 and a water content of 20.1%. The introduction of dolomite was aimed at improving these properties. The results for the experiments conducted at WHSV 5, 2.5 and 1.67 suggested that the bio-oil quality deteriorated even further. This is indicated by the HHV, carbon and water content measurements shown in Table 5. For instance, the increase in water content can be explained primarily by the enhanced dehydration reactions. Such increase in water content was also reported when CaO was applied to catalyze pyrolysis vapors of pine powder in a fluidized bed reactor [52]. It must be also noted that there was no phase separation in the bio-oil obtained from these experiments and the results are a reflection of total oil collected. The data from the CO_2 breakthrough curve also suggested that the major portion of these experiments were streamed well beyond the fast carbonation stage resulting in a bed with dolomite which is partially or fully deactivated for the remainder of the experiment. Here within we postulate, that the carbonate product layer formed as a result of CaO carbonation limits the diffusion of the pyrolysis vapors to the active sites available for deoxygenation and this results in a bio-oil with undesirable quality. Essentially it means that sluggish CO_2 sorption stage was ongoing, as the dolomite was no longer able to deoxygenate the pyrolysis vapors.

Such drastic changes in the properties of the liquid product were also observed during steam reforming of raw bio-oil as a result of the CaO carbonation [53]. Furthermore, in a fluidized bed setup it is very likely that dolomite surface properties are modified due to contact with biomass particles and high gas flowrates or velocities leading to reduced activity over time and thus modifying the bio-oil quality. It has been also reported that coke and ash from the biomass can be deposited on the active sites of dolomite during steam gasification [54]. On the other hand for the experiments conducted at WHSV 1.25 and 0.83, there was a visible phase separation in the collected bio-oil and thus it was possible to analyze the useful organic phase (see supplement for photo). It is generally accepted that this bio-oil has an immense potential as a renewable feedstock and it often reported as such in the literature [34,35]. The analysis showed that the oxygen content reduced to 27.0 and 23.8 wt% respectively. Moreover HHV increased to 25.8 and 27.1 MJ/kg on as received basis respectively. Further, the pH of the bio-oil improved to great extent up to 6.0 $\pm$ 0.03 at WHSV 0.83. It will also be shown later by GC–MS analysis that the acidic compounds decreased substantially.

Nevertheless, a low bio-oil yield of 20.0% and a non CO_2 free pyrolysis gas at WHSV 0.83 opened up scope for further optimization of the catalytic pyrolysis process. The loss of bio-oil yield can be explained by the intensified secondary cracking reactions over the partially saturated dolomite in the bed over the duration of the experiment. Data from the run at WHSV 1.25 suggests that it is ideal in terms of obtaining an organic rich bio-oil with substantial bio-oil yield. It is also clear that the experimental time needs to be optimized in order not to go beyond the fast carbonation stage to obtain a CO_2 free gas. As a result a final optimized experiment was carried out with WHSV 1.25 and experimental time 30 mins which is equal to the CO_2 breakthrough time at WHSV 1.25. Other relevant parameters remained unchanged. As a result, an organic rich bio-oil with an oxygen content of reduced up to 21.56 wt% and a HHV of 28.01 MJ/g on as received basis was obtained. This is significantly higher than those reported in the literature. For example
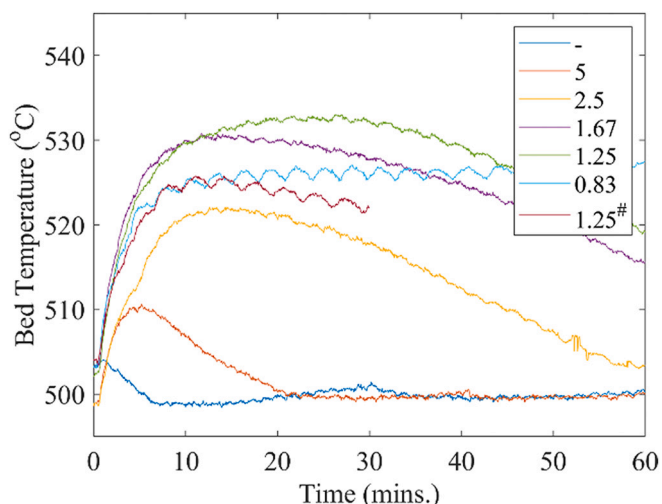

Fig. 5. Fluidized bed temperature profiles for varying WHSV.

Table 5

Physio chemical properties of catalytic bio-oil in comparion to non-catalytic bio-oil for different WHSV.

	Non-Catalytic [a]	WHSV 5[a]	WHSV 2.5[a]	WHSV 1.66 [a]	WHSV 1.25[b]	WHSV 0.83[b]	WHSV 1.25# [b]
Run time (Mins.)	60	60	60	60	60	60	30
H_2O content (%)	20.13	23.81	35.86	56.03	–	–	–
H_2O content (%) Organic Phase	–	–	–	–	5.23	5.45	5.61
H_2O content (%) Aqueous Phase	–	–	–	–	92.85	93.86	92.40
pH	3.0	3.2	3.4	3.4	5.3	6.0	6.0
C (wt% arb.)	45.69	45.87	35.33	20.40	64.76	67.76	70.01
H (wt% arb.)	7.37	7.85	8.06	9.60	7.35	7.52	7.55
N (wt% arb.)	0.60	0.55	0.49	0.71	0.87	0.88	0.88
O[c] (wt% arb.)	46.34	45.73	56.12	69.69	27.01	23.84	21.56
O/C[d]	0.76	0.75	1.19	2.55	0.31	0.26	0.23
H/C[d]	1.66	2.04	2.72	5.61	1.35	1.32	1.29
HHV[e] (MJ/kg, arb.)	18.12	18.25	16.90	12.32	25.80	27.11	28.01

[a] Non-separable organic and aqueous phases.
[b] Organic Phase (2 Phase Oil).
[c] By Difference.
[d] mol/mol.
[e] As received basis (arb.), measured on bomb calorimeter.

when tulip tree was pyrolyzed under the influence of dolomite at 500 °C, the HHV was 26.65 MJ/kg and the oxygen content was 30.64 wt% [35]. Overall, these results are a representation of a batch process where the characteristics of the dolomite within the fluidized bed is changing with time. In practice it is possible to continuously feed fresh dolomite along with the biomass and this may further reveal improvements in the bio-oil yield. Circulating fluidized bed or FCC reactors are often recommend for such operations as they also allow for continuous catalyst regeneration.

3.2.4. Chemical composition of the bio-oil

To further substantiate the physio-chemical properties of the organic rich bio-oil, GCMS analysis was performed for the organic phase of the samples collected from the experiments conducted at WHSV 1.25, 0.83 and 1.25# and the list of the chemical compounds detected are provided in the Table 1s and 2s of the supplement. Fig. 6 shows the relative proportions of the different groups in the non-catalytic bio-oil compared to the catalytic bio-oil. In comparison to the GCMS results of the non-catalytic bio-oil, the application of dolomite resulted in a drastic reduction in the yeilds of acids, anydrosugars and aldehydes of the bio-oil. Where as the relative yields of ketones and phenols drastically increased. Other oxygenates such as furans and alochols remained more or less unaffected and the hydrocarbon content slightly increased.
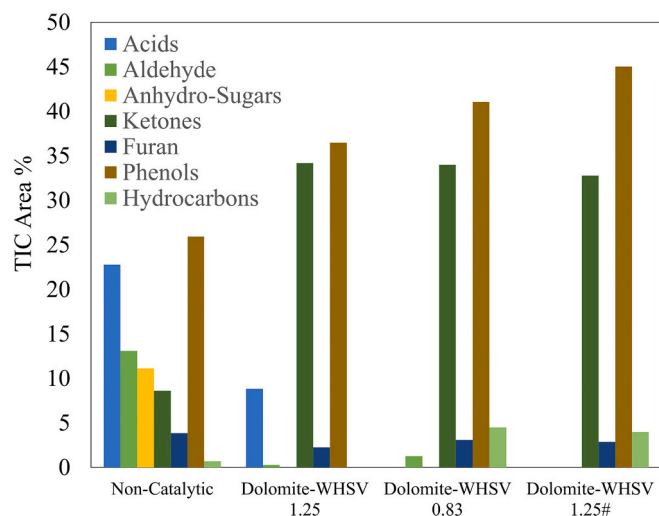
Fig. 6. GCMS analysis of catalytic bio-oil for WHSV 1.25, 0.83 and 1.25# compared to non-catalytic pyrolysis.

In this investigation, acetic acid and 4-hydroxy-3-methoxy-benzoic acid were the primary acidic products detected during non catalytic pyrolysis. The application of dolomite at WHSV 1.25 drastically reduced the acidic content and it was completley eliminated when WHSV was 0.83 and 1.25#. This is supported by the higher pH value. This reduction in acids can be explained by the ability of CaO to directly fix the acidic compounds and their quasi-CO_2 intermediates [52]. The complele elimination of anhydrosugars such as 1,6-Anhydro-ß-D-mannopyranose was also very noticeable for all the cases. This may be explained by the ring opening reactions possibly promoted by dolomite. Typically the glycosidic linkages between the pyranose rings of polymeric carbohydrate molecules were cracked leading to formation of other oxygenates or charring. Piskorz et al. [55] reported such a mechanism for lignocellulose biomass.

Further, both linear and cyclic ketones were enhanced in all the cases. In general, dehydration reactions of cellulose and hemicellulose promote formation of such products and therefore it can be stated that dolomite promoted dehydration reactions during pyrolysis. The major linear ketones identified were acetone and 2-pentanone. The increase in the formation of pentanones could be ascribed to the strong basic sites on CaO and MgO which promote aldol condensation reactions. Moreover, abundance of methyl- or ethyl-substituted cyclopentenones increased while the hydroxy-methyl substituted cyclopentenones were reduced. This is beneficial as oxygen containg hydroxy group was eliminated from the cyclopentenones. The total relative abundance of such products also increased when nano oxides of CaO and MgO were used as catalyst for pyrolysis of poplar wood [56]. Ketonization of acids to form ketones are also known to be active on basic sites of calcium based catalysts [57,58]. This also suggests that the elimination of carboxylic acids was a consequence of ketonization.

Non-catalytic experiment also produced bulkier phenols such as syringol, guaiacol and eugenol which contain methoxyl group and/or unsaturated C—C bonds on the side chain. Analysis of the catalytic experimental data revealed that dolomite was effective in reforming both methoxyl group and unsaturated side chain. As a result, relative abundance of phenols and alkyl-phenols were enhanced. Lin et al., 2010 [52] reported that the use of calcium based catalyst led to the dominance of direct demethoxylation pathway in enhancing the phenols and alkyl-phenols. It is also possible that the increase in alkylated phenols was possible due to reaction with methenium ion and methylene radicals formed during the demethoxylation process of guaiacyl monomers. Overall, the transformation of bulkier phenols to alkylated phenols is beneficial due to their lower oxygen content and also due to their influence on decreasing the viscosity of the bio-oil. Furthermore, a slight increase in aliphatic hydrocarbons was also detected. In conclusion, bio-

oil with HHV of 28.0 MJ/kg (as received), pH of 6 was obtained. It mainly contained methyl substituted cyclopentenones and alkyl-phenols with minor abundance of hydrocarbons. Summarizing, the literature results as cited previously are compared to the present research and are tabulated in Table 6.

3.2.5. Hydrogen

The application of dolomite significantly eliminated the oxygen containing components in the bio-oil in comparison to non-catalytic pyrolysis. However, downstream hydrogen based processes may be still required to meet the specifications of a bio based refinery. During such processes, various reactions such as hydrogenation, hydro-deoxygenation, hydrocracking, decarboxylation, decarbonylation and polymerization are promoted depending on process conditions and the choice of the catalyst [60]. The general objective of such a process is to limit the oxygen content of the product to less than 1% to realize compatibility with hydrocarbon fuels [61]. In this context, it is desirable to selectively promote hydrodeoxygenation reaction and limit hydrogenation of unsaturated bonds to limit the required hydrogen amounts to achieve full de-oxygenation. Furthermore it is desirable to limit decarboxylation and decarbonylation reactions to conserve the carbon in the end product. Approximate stoichiometric requirement of hydrogen is about 31 to 44 mol of hydrogen per kg of pyrolysis oil [15]. However, in practice, an excess hydrogen of 100%- 200% may be required in order to maintain a high hydrogen partial pressure. Therefore the source of hydrogen is a very vital factor determining the sustainability and economic feasibility of such a hydrogen-based process.

Hydrogen can be acquired via externally and/or internal routes. External processes such as steam reforming of methane, heavy oil oxidation, thermochemical decomposition of water, steam gasification of coal and biomass can provide hydrogen [62]. Contrary to external sources of hydrogen, the hydrogen generated by dolomite as a consequence of shift in the WGS reaction equilibrium can possibly meet the requirement. Here we would like to quantify the hydrogen generated and answer the question if it can fulfil the requirement.

In this investigation, it was shown that the application of dolomite can simultaneously generate a moderately deoxygenated organic rich bio-oil and CO_2 free hydrogen rich gas when the WHSV was 1.25 and run time was 30 min. The bio-oil contained 21.56 wt% oxygen amounting to 0.32 mol on total feed basis. When HDO reaction is promoted selectively (ignoring hydrogenation side reactions), oxygen in the bio-oil is removed in the form of water. Stoichiometrically two hydrogen atoms are necessary to remove one oxygen atom in the form of water ($O + 2H \rightarrow H_2O$). That means 0.32 mol of H_2 is required and based on the data, 0.86 mol of H_2 is available. This is around 2.65 times the stoichiometric requirement. Similarly it can be calculated that 3.4 mol of H_2 can be generated for 1 Kg biomass input for a requirement of 1.27 mol to fully deoxygenate the organic phase. So in conclusion it can be stated that the here prescribed catalytic pyrolysis process with dolomite can deliver enough H_2 for downstream processing.

3.3. CO₂ sorbent-catalyst characterization

The raw dolomite was characterized by applying TGA, XRD and BET Analysis. The thermogravimetric (TG) (weight loss, %) and the derivative thermogravimetric (DTG) (derivative weight loss, %/°C) profiles resulting from thermal decomposition of the raw dolomite are depicted in Fig. 7. It is observed that decomposition of this dolomite takes place in the 425–800 °C range, which is ascribed to direct transformation into CaO and MgO. The dolomite calcination process occurred following Eq. 1. The results reveal that the highest mass loss occurred at 800 °C, and there is no mass loss above 800 °C.

$$CaMg(CO_3)_2 \rightarrow CaO + MgO + 2CO_2 \tag{1}$$

XRD analysis was performed to obtain additional insight into the characteristics of dolomite as shown in Fig. 8. The XRD pattern of raw dolomite revealed a prevailing peak of calcium magnesium carbonate ($CaMg (CO_3)_2$) at $2\theta = 31.1°$. Moreover, other less intense peaks corresponding to calcium magnesium carbonate and small peaks of calcium carbonate ($CaCO_3$) were are also detected. On the contrary, XRD pattern of calcined dolomite showed diffraction peaks revenant of calcium oxide (CaO) at $2\theta = 37.6°$ and magnesium oxide (MgO) at $2\theta = 43.2°$. Further, the peaks corresponding to $CaMg(CO3)_2$ were not revealed by the XRD analysis and thus confirmed the calcination process at 800 °C in flowing air leading to formation of CaO and MgO species. Consequently morphology of the calcined dolomite differed significantly in

Table 6
Relevant literature on catalytic biomass pyrolysis in fluidized bed reactor in comparison to present investigation.

Reference	Feedstock	Catalyst	Pyrolysis Temp.	Total Bio-Oil Yield (wt%)	Char Yield (wt %)	Gas Yield (wt %)	Mass Balance (wt %)	HHV (MJ/ kg)	pH
Beechwood pyrolysis in fludized bed reactor									
[38]	Beechwood	–	475	62.7	10.2	22.6	95.5	23.4[a]	2.5
[39]	Beechwood	–	500	65.0	15.9	17.7	98.6	–	–
[40]	Beechwood	–	500	61.6	15.6	17.4	94.6	–	–
Present work	Beechwood	–	500	61.1	12.8	15.1	89.0	18.1[b]	3.0
In-situ catalysts in fludized bed for pyrolysis									
[43]	White oak	Ca²⁺Zeolite	500	30	13	27	70	14.2[b]	2.9
		β Zeolite		29	24	14	67	10.0[b]	2.6
[44]	Corncob	FCC	550	45.0	30.0	21.8	97.8	34.2[a]	5.1
[45]	Piniyon	HZSM5	475	49.3	20.9	29.6	100	28.5[a]	2.8
	Juniper	Redmud		44.3	23.5	32.1	100	29.4[a]	3.5
[46]									
[59]	Bamboo	HZSM5	475	49.1	25.7	25.1	100	27.9[a]	3.7
		Redmud		50.3	25.5	24.0	100	27.2[a]	3.9
Dolomite as in-situ catalyst for biomass pyrolysis									
[34][c]	Forest-Pine	Dolomite	450	48	26	26	100	29.6[a]	4.6
[35]	Tulip Tree	Dolomite	500	40.4	26.4	33.0	100	26.55[a]	5.8
[47]	Food waste	Dolomite	500	38.8	41.9	19.2	100	34.7[a]	4.3
Present work, WHSV 1.25[#]	Beechwood	Dolomite	500	25.2	48.8[d]	10.8[e]	87.8	28.0[b]	6.0

[a] HHV reported on dry basis.
[b] HHV reported on as received basis.
[c] Auger Reactor.
[d] Including Heterogenous Char (Coke + CO₂ Captured).
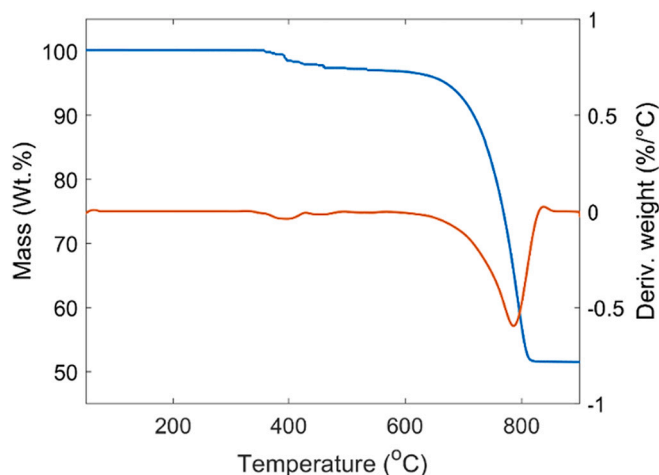[e] Gas free of CO₂.

Fig. 7. Thermogravimetric analysis of raw dolomite.
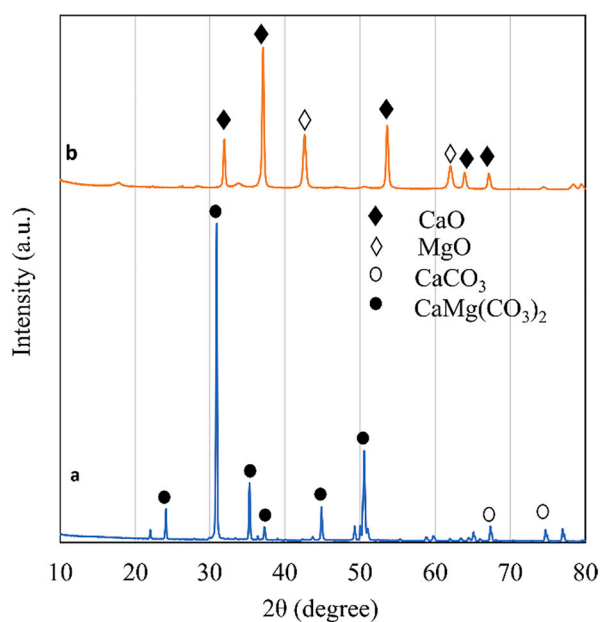

Fig. 8. X-Ray diffraction (XRD) patterns of (a) raw dolomite and (b) calcined dolomite.

comparison to the raw dolomite. The BET surface area (S_{BET}) of calcined dolomite catalyst was measured to be 10.58 m^2/g in comparison to 1.72 m^2/g for raw dolomite. The enhancement of the surface area is a result of CO_2 release during calcination which in turn formed orderly pores with more porosity on the surface of calcined dolomite. Overall, both chemical composition and the physical properties were modified as a consequence of calcination.

3.4. Analysis of spent dolomite

The mass of carbon captured by the dolomite comprises of the amount of CO_2 adsorbed and the coke deposited. The TA Instruments Q5550 was employed with the objective of quantifying both the amount of coke deposited and CO_2 captured during each experimental run. For this purpose, sample of bed material collected form the fluidized bed post experiments were subjected to analysis on TGA. In order to desorb CO_2, the samples were heated from 30 °C to 900 °C at 50 °C/min followed by an isothermal stage for 5 min under inert atmosphere (30 ml/min N_2). Finally, the temperature was ramped down to 800 °C at 50 °C/

min and held for 30 mins in air (30 ml/min air) to oxidize the deposited coke. The thermogravimetric (TG) and the derivative thermogravimetric (DTG) profiles resulting from both desorption stage and oxidizing stage are shown in Fig. 9 (a). The profiles comprise of two distinct weight loss stages and the first weight loss can be ascribed to CO_2 desorption from the dolomite. The second weight loss corresponds to removal of coke deposited on the surface of the dolomite.

Both coke deposited and CO_2 captured were quantified for all the experiments and are graphically represented in Fig. 9 (b). Calcined dolomite has a stoichiometric CO_2 capture capacity of 0.46 g/g and it became nearly saturated by CO_2 sorption up to a WHSV of 2.5. For example, the CO_2 desorbed from the samples were measured to be 0.45 and 0.42 g/g when WHSV was 5 and 2.5 respectively. Beyond WHSV 2.5, the analysis showed that the calcined dolomite was not fully saturated and still active for CO_2 sorption. This also corresponds to the CO_2 breakthrough curves as discussed earlier. Moreover, the total CO_2 captured on total feed basis increased with increased loading. The captured CO_2 can be attributed to both primary decomposition of holocellulose and deoxygenation reactions. Deoxygenation reactions such as Ketonization are known to release CO_2. Moreover at WHSV 1.25[#] the saturation level of calcined dolomite in the bed was only about 30% of stoichiometry and consequently more active sites were available for deoxygenation and thus a moderately deoxygenated oil was obtained. The total coke deposited also increased with increased loading.

Moreover an XRD analysis was performed to gain further insight into the diffraction patterns of spent dolomite in comparison to calcined dolomite. Samples from experiments at WHSV 5 and 1.25[#] were selected for XRD analysis and the diffraction patterns are shown in Fig. 10. These samples were selected with an aim to draw out a contrast between experiments yielding the least and best results in terms of gas an bio-oil quality. As described earlier, diffraction peaks ascribed to CaO and MgO were predominant for the calcined dolomite. The presence of $CaCO_3$ was revealed in all the spent samples and hence it further substantiates the carbonation reaction. The presence of CaO was also detected in the spent dolomite samples and thus revealing that they were not fully saturated of $CaCO_3$. Nevertheless, the intensity and abundance of the CaO peaks were least for the sample from WHSV 5 and thus revealing that the extent of carbonation was much higher in comparison to WHSV 1.25[#]. Moreover, this compared well with the TGA analysis of spent dolomite samples. Magnesium very much remained in the oxide phase but it exhibited slightly broader peaks for WHSV 5 in comparison to WHSV 1.25[#]. This indicated that over an extended run time the sample from WHSV 5 underwent only slight attrition.

In order to further examine the state of the spent dolomite in comparison to the calcined dolomite, scanning electron microscope (SEM) scans were extracted. Similar to XRD analysis, samples from experiments at WHSV 5 and 1.25[#] were selected. In Fig. 11, the SEM scans for both the calcined dolomite and spent dolomite samples are illustrated and they appear to have significant differences. Fig. 11 (a) reveals that the calcined dolomite has a simple cubic structure with irregular surface formed by small clusters of grains lying on other larger ones. SEM scan of the sample from WHSV 1.25[#] as shown in Fig. 11 (b) reveals a noticeable change in the texture of the surface as the grains appeared to have been reduced in comparison to calcined dolomite. Moreover, the appearance of cracks on the surface is also very evident and interestingly it could have prevented the blockage of the pores and maintained the diffusion of CO_2 and pyrolysis vapors to the interior of the particle. This also substantiates the results from the experiment conducted at WHSV 1.25[#]. On the contrary, the sample from WHSV 5 reveals a structure which has undergone slight fragmentation as seen in Fig. 11 (c). Moreover, the surface appears to have been covered completely with carbonate product layer and coke. This means that the access to the active sites were limited resulting in an undesirable bio-oil and gas product. Similarly, Hervy et al. [54] found ash and coke deposits on dolomite when used as bed material in gasification and concluded that the availability of the active sites were lowered.
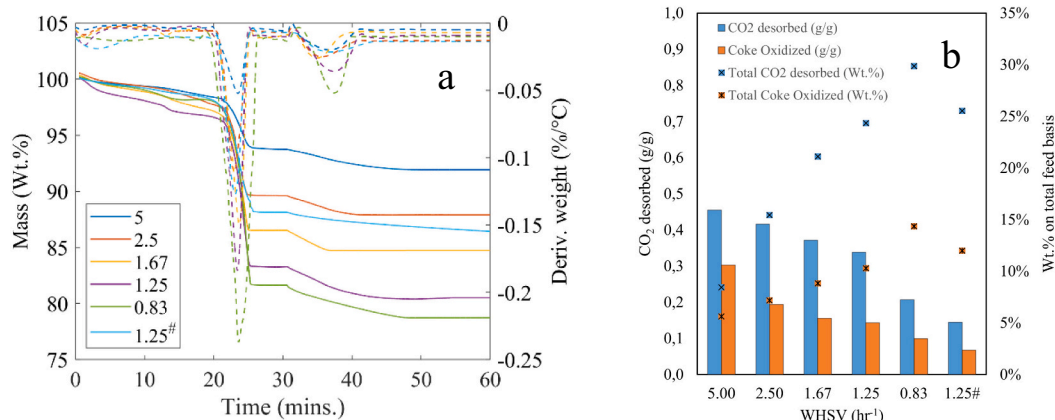
Fig. 9. (a) Thermogravimetric analysis of spent dolomite (b) quantitative analysis of CO_2 adsorbed and coke deposited.
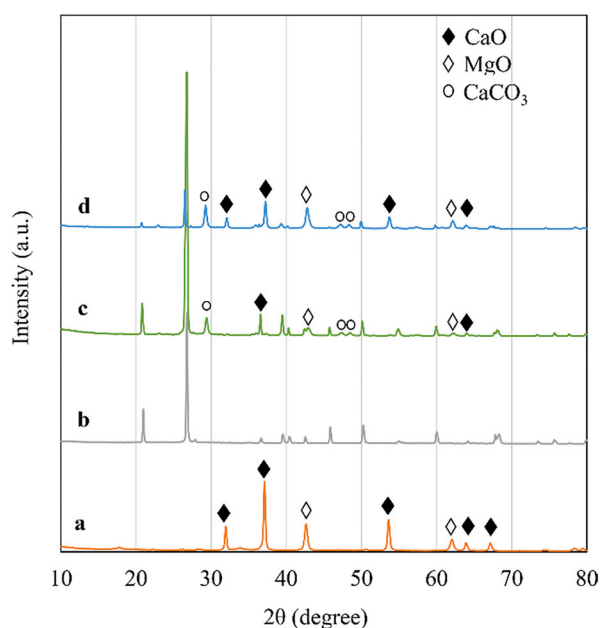

Fig. 10. X-Ray diffraction (XRD) patterns of (a) calcined dolomite and (b) Quartz sand (C) Spent Dolomite WHSV 5 (d) Spent Dolomite WHSV 1.25

4. Conclusion

The influence of dolomite on fast pyrolysis behavior of beechwood was investigated with a bench scale bubbling fluidized-bed reactor at a pyrolysis temperature of 500 °C and varying catalyst loading (WHSV). The results reveal that a moderately deoxygenated bio-oil and CO_2 free pyrolysis gas can be produced simultaneously. Overall, the oxygen content of the organic rich bio-oil reduced to 21.5 wt% from 47.3 wt% and the heating value of 28.0 MJ/kg (as received) were obtained. These results were obtained when the rapid carbonation stage was prevailing throughout the run. On the other hand, the onset of the sluggish carbonation stage impacted the bio-oil quality negatively and also added CO_2 to the pyrolysis gas.

Overall, dolomite was effective in transforming the complex mixture of oxygenates generated during pyrolysis into a mixture of intermediate compounds with a considerable reduction in oxygen content. This is a direct impact of the basic sites contained in the dolomite and stable process conditions throughout the run time. Acids and anhydro-sugars which majorly contribute to the acidity of the bio-oil were completely eliminated. The relative yield of cresols increased from 0.4% to 23.3% and the relative yield cyclopentanones were increased from 3% to 29.6%. These intermediate compounds present in the bio-oil tend to be more stable and hence it is much more feasible to further upgrade this bio-oil. For example cyclopentanones are useful intermediates which can undergo aldol condensation and hydrogenation reactions to generate longer chain hydrocarbons as described in literature. Additionally, cresols are known to be precursors for the generation of hydrocarbons via a reaction pathway which is dependent on the type of catalyst and its characteristics. It was also calculated that 0.86 mol of in situ H_2 was generated which is almost 2.65 times the requirement for further downstream deoxygenation. Thus this research unravelled the potential of dolomite as a in situ deoxygenation catalyst and CO_2 sorbent to simultaneous upgrade the raw pyrolysis vapors and produce a CO_2 free H_2 rich gas for fast pyrolysis of beechwood. Further, it opens up possibility to investigate downstream upgrading of moderately deoxygenated vapors with in-situ H_2 over a suitable catalyst.
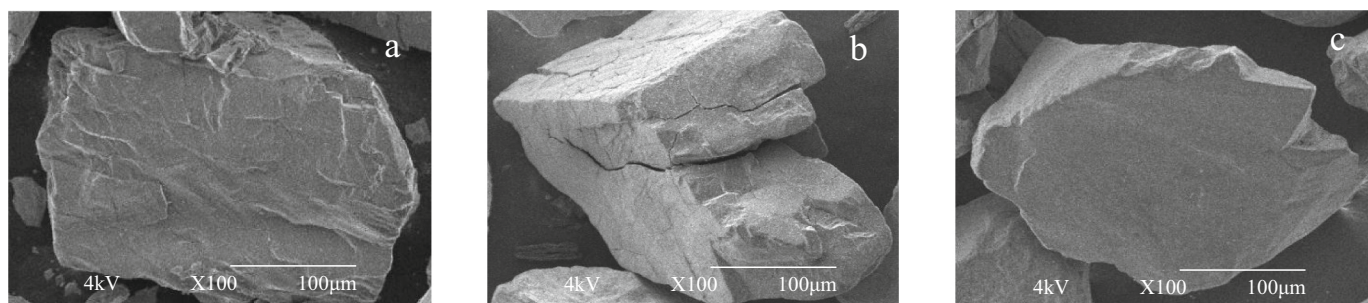

Fig. 11. SEM images of (a) Calcined dolomite (b) Spent Dolomite WHSV 1.25# and (c) Spent Dolomite WHSV 5.

Declaration of Competing Interest

Acknowledgements

Appendix A. Supplementary data

Supplementary data to this article can be found online at https://doi.org/10.1016/j.fuproc.2021.107029.

References

[1] F. Creutzig, N.H. Ravindranath, G. Berndes, S. Bolwig, R. Bright, F. Cherubini, H. Chum, E. Corbera, M. Delucchi, A. Faaij, J. Fargione, H. Haberl, G. Heath, O. Lucon, R. Plevin, A. Popp, C. Robledo-Abad, S. Rose, P. Smith, A. Stromman, S. Suh, O. Masera, Bioenergy and climate change mitigation: an assessment, GCB Bioenergy (2015), https://doi.org/10.1111/gcbb.12205.

[2] K. Lorenz, R. Lal, Carbon Sequestration in Agricultural Ecosystems, 2018, https://doi.org/10.1007/978-3-319-92318-5.

[3] K. Van Meerbeek, B. Muys, M. Hermy, Lignocellulosic biomass for bioenergy beyond intensive cropland and forests, Renew. Sust. Energ. Rev. (2019), https://doi.org/10.1016/j.rser.2018.12.009.

[4] A. Rödl, Lignocellulosic biomass, in: Biokerosene Status Prospect, 2017, https://doi.org/10.1007/978-3-662-53065-8_9.

[5] S.S. Hassan, G.A. Williams, A.K. Jaiswal, Lignocellulosic biorefineries in Europe: current state and prospects, Trends Biotechnol. (2019), https://doi.org/10.1016/j.tibtech.2018.07.002.

[6] D. Mohan, C.U. Pittman, P.H. Steele, Pyrolysis of wood/biomass for bio-oil: a critical review, Energy Fuel (2006), https://doi.org/10.1021/ef0502397.

[7] A.V. Bridgwater, Principles and practice of biomass fast pyrolysis processes for liquids, J. Anal. Appl. Pyrolysis (1999), https://doi.org/10.1016/S0165-2370(99)00005-4.

[8] D. Meier, O. Faix, State of the art of applied fast pyrolysis of lignocellulosic materials - a review, Bioresour. Technol. (1999), https://doi.org/10.1016/S0960-8524(98)00086-8.

[9] N.H. Leibbrandt, J.H. Knoetze, J.F. Görgens, Comparing biological and thermochemical processing of sugarcane bagasse: an energy balance perspective, Biomass Bioenergy (2011), https://doi.org/10.1016/j.biombioe.2011.02.017.

[10] S. Czernik, A.V. Bridgwater, Overview of applications of biomass fast pyrolysis oil, Energy Fuel (2004), https://doi.org/10.1021/ef034067u.

[11] J. Fermoso, P. Pizarro, J.M. Coronado, D.P. Serrano, Advanced biofuels production by upgrading of pyrolysis bio-oil, Wiley Interdisc. Energy Environ. (2017), https://doi.org/10.1002/wene.245.

[12] M. Stöcker, Biofuels and biomass-to-liquid fuels in the biorefinery: catalytic conversion of lignocellulosic biomass using porous materials, Angew. Chem. Int. Ed. (2008), https://doi.org/10.1002/anie.200801476.

[13] D.M. Alonso, J.Q. Bond, J.A. Dumesic, Catalytic conversion of biomass to biofuels, Green Chem. (2010), https://doi.org/10.1039/c004654j.

[14] R.H. Venderbosch, A critical view on catalytic pyrolysis of biomass, ChemSusChem, (2015), https://doi.org/10.1002/cssc.201500115.

[15] A.V. Bridgwater, Production of high grade fuels and chemicals from catalytic pyrolysis of biomass, Catal. Today (1996), https://doi.org/10.1016/0920-5861(95)00294-4.

[16] I.A. Vasalos, A.A. Lappas, E.P. Kopalidou, K.G. Kalogiannis, Biomass catalytic pyrolysis: process design and economic analysis, Wiley Interdisc. Rev. Energy Environ. (2016), https://doi.org/10.1002/wene.192.

[17] C. Liu, H. Wang, A.M. Karim, J. Sun, Y. Wang, Catalytic fast pyrolysis of lignocellulosic biomass, Chem. Soc. Rev. (2014), https://doi.org/10.1039/c3cs60414d.

[18] S. Kelkar, C.M. Saffron, K. Andreassi, Z. Li, A. Murkute, D.J. Miller, T.J. Pinnavaia, R.M. Kriegel, A survey of catalysts for aromatics from fast pyrolysis of biomass, Appl. Catal. B Environ. (2015), https://doi.org/10.1016/j.apcatb.2015.02.020.

[19] G. Kabir, B.H. Hameed, Recent progress on catalytic pyrolysis of lignocellulosic biomass to high-grade bio-oil and bio-chemicals, Renew. Sust. Energ. Rev. (2017), https://doi.org/10.1016/j.rser.2016.12.001.

[20] E.F. Iliopoulou, K.S. Triantafyllidis, A.A. Lappas, Overview of catalytic upgrading of biomass pyrolysis vapors toward the production of fuels and high-value chemicals, Wiley Interdisc. Rev. Energy Environ. (2019), https://doi.org/10.1002/wene.322.

[21] J. Jae, G.A. Tompsett, A.J. Foster, K.D. Hammond, S.M. Auerbach, R.F. Lobo, G.W. Huber, Investigation into the shape selectivity of zeolite catalysts for biomass conversion, J. Catal. (2011), https://doi.org/10.1016/j.jcat.2011.01.019.

[22] D.J. Mihalcik, C.A. Mullen, A.A. Boateng, Screening acidic zeolites for catalytic fast pyrolysis of biomass and its components, J. Anal. Appl. Pyrolysis (2011), https://doi.org/10.1016/j.jaap.2011.06.001.

[23] J. Liang, G. Shan, Y. Sun, Catalytic fast pyrolysis of lignocellulosic biomass: critical role of zeolite catalysts, Renew. Sust. Energ. Rev. (2021), https://doi.org/10.1016/j.rser.2021.110707.

[24] H. Hernando, A.M. Hernández-Giménez, C. Ochoa-Hernández, P.C.A. Bruijnincx, K. Houben, M. Baldus, P. Pizarro, J.M. Coronado, J. Fermoso, J. Čejka, B.M. Weckhuysen, D.P. Serrano, Engineering the acidity and accessibility of the zeolite ZSM-5 for efficient bio-oil upgrading in catalytic pyrolysis of lignocellulose, Green Chem. (2018), https://doi.org/10.1039/c8gc01722k.

[25] M. Asadieraghi, W.M. Ashri Wan Daud, H.F. Abbas, Heterogeneous catalysts for advanced bio-fuel production through catalytic biomass pyrolysis vapor upgrading: a review, RSC Adv. (2015), https://doi.org/10.1039/c5ra00762c.

[26] V. Paasikallio, C. Lindfors, E. Kuoppala, Y. Solantausta, A. Oasmaa, J. Lehto, J. Lehtonen, Product quality and catalyst deactivation in a four day catalytic fast pyrolysis production run, Green Chem. (2014), https://doi.org/10.1039/c4gc00571f.

[27] H. Li, Y. Wang, N. Zhou, L. Dai, W. Deng, C. Liu, Y. Cheng, Y. Liu, K. Cobb, P. Chen, R. Ruan, Applications of calcium oxide–based catalysts in biomass pyrolysis/gasification – a review, J. Clean. Prod. (2021), https://doi.org/10.1016/j.jclepro.2021.125826.

[28] A. Orío, J. Corella, I. Narváez, Characterization and activity of different dolomites for hot gas cleaning in biomass gasification, Dev. Thermochem. Biomass Convers. (1997), https://doi.org/10.1007/978-94-009-1559-6_92.

[29] J. Corella, J.M. Toledo, R. Padilla, Olivine or dolomite as in-bed additive in biomass gasification with air in a fluidized bed: which is better? Energy Fuel (2004) https://doi.org/10.1021/ef0340918.

[30] C. Berrueco, D. Montané, B. Matas Güell, G. del Alamo, Effect of temperature and dolomite on tar formation during gasification of torrefied biomass in a pressurized fluidized bed, Energy (2014), https://doi.org/10.1016/j.energy.2013.12.035.

[31] G. Hu, S. Xu, S. Li, C. Xiao, S. Liu, Steam gasification of apricot stones with olivine and dolomite as downstream catalysts, Fuel Process. Technol. (2006), https://doi.org/10.1016/j.fuproc.2005.07.008.

[32] M.W. Islam, A review of dolomite catalyst for biomass gasification tar removal, Fuel (2020), https://doi.org/10.1016/j.fuel.2020.117095.

[33] K. Johnsen, H.J. Ryu, J.R. Grace, C.J. Lim, Sorption-enhanced steam reforming of methane in a fluidized bed reactor with dolomite as CO2-acceptor, Chem. Eng. Sci. (2006), https://doi.org/10.1016/j.ces.2005.08.022.

[34] A. Veses, M. Aznar, I. Martínez, J.D. Martínez, J.M. López, M.V. Navarro, M.S. Callén, R. Murillo, T. García, Catalytic pyrolysis of wood biomass in an auger reactor using calcium-based catalysts, Bioresour. Technol. (2014), https://doi.org/10.1016/j.biortech.2014.03.146.

[35] H.V. Ly, D.H. Lim, J.W. Sim, S.S. Kim, J. Kim, Catalytic pyrolysis of tulip tree (Liriodendron) in bubbling fluidized-bed reactor for upgrading bio-oil using dolomite catalyst, Energy (2018), https://doi.org/10.1016/j.energy.2018.08.001.

[36] W. Charusiri, T. Vitidsant, et al., Sustain. Chem. Pharm. (2017), https://doi.org/10.1016/j.scp.2017.10.005.

[37] E. Schröder, Experiments on the pyrolysis of large beechwood particles in fixed beds, J. Anal. Appl. Pyrolysis (2004), https://doi.org/10.1016/j.jaap.2003.09.004.

[38] A.M. Azeez, D. Meier, J. Odermatt, T. Willner, Fast pyrolysis of African and European lignocellulosic biomasses using Py-GC/MS and fluidized bed reactor, Energy Fuel (2010), https://doi.org/10.1021/ef9012856.

[39] X. Wang, S.R.A. Kersten, W. Prins, W.P.M. Van Swaaij, Biomass pyrolysis in a fluidized bed reactor. Part 2: experimental validation of model results, Ind. Eng. Chem. Res. (2005), https://doi.org/10.1021/ie050486y.

[40] E. Hoekstra, K.J.A. Hogendoorn, X. Wang, R.J.M. Westerhof, S.R.A. Kersten, W.P.M. Van Swaaij, M.J. Groeneveld, Fast pyrolysis of biomass in a fluidized bed reactor: in situ filtering of the vapors, Ind. Eng. Chem. Res. (2009), https://doi.org/10.1021/ie8017274.

[41] A. Domínguez, J.A. Menéndez, M. Inguanzo, P.L. Bernad, J.J. Pis, Gas chromatographic-mass spectrometric study of the oil fractions produced by microwave-assisted pyrolysis of different sewage sludges, J. Chromatogr. A (2003), https://doi.org/10.1016/S0021-9673(03)01176-2.

[42] N. Marin, S. Collura, V.I. Sharypov, N.G. Beregovtsova, S.V. Baryshnikov, B.N. Kutnetzov, V. Cebolla, J.V. Weber, Copyrolysis of wood biomass and synthetic polymers mixtures. Part II: characterisation of the liquid phases, J. Anal. Appl. Pyrolysis (2002), https://doi.org/10.1016/S0165-2370(01)00179-6.

[43] C.A. Mullen, A.A. Boateng, D.J. Mihalcik, N.M. Goldberg, Catalytic fast pyrolysis of white oak wood in a bubbling fluidized bed, Energy Fuel (2011), https://doi.org/10.1021/ef201286z.

[44] H. Zhang, R. Xiao, D. Wang, Z. Zhong, M. Song, Q. Pan, G. He, Catalytic fast pyrolysis of biomass in a fluidized bed with fresh and spent fluidized catalytic cracking (FCC) catalysts, Energy Fuel (2009), https://doi.org/10.1021/ef900720m.

[45] B.K. Yathavan, F.A. Agblevor, Catalytic pyrolysis of pinyon-juniper using red mud and HZSM-5, Energy Fuel (2013), https://doi.org/10.1021/ef401853a.

[46] H. Zhang, R. Xiao, H. Huang, G. Xiao, Comparison of non-catalytic and catalytic fast pyrolysis of corncob in a fluidized bed reactor, Bioresour. Technol. (2009), https://doi.org/10.1016/j.biortech.2008.08.031.

[47] H.V. Ly, Q.K. Tran, S.S. Kim, J. Kim, S.S. Choi, C. Oh, Catalytic upgrade for pyrolysis of food waste in a bubbling fluidized-bed reactor, Environ. Pollut. (2021), https://doi.org/10.1016/j.envpol.2020.116023.

[48] D. Mess, A.F. Sarofim, J.P. Longwell, Product layer diffusion during the reaction of calcium oxide with carbon dioxide, Energy Fuel (1999), https://doi.org/10.1021/ef980266f.

[49] B. Dou, Y. Song, Y. Liu, C. Feng, High temperature CO2 capture using calcium oxide sorbent in a fixed-bed reactor, J. Hazard. Mater. (2010), https://doi.org/10.1016/j.jhazmat.2010.07.091.

[50] S.D. Kenarsari, Y. Zheng, CO2 capture using calcium oxide under biomass gasification conditions, J. CO2 Util. (2015), https://doi.org/10.1016/j.jcou.2014.11.001.

[51] D.L. Elllg, C.K. Lai, D.W. Mead, J.P. Longwell, W.A. Peters, Pyrolysis of volatile aromatic hydrocarbons and n-heptane over calcium oxide and quartz, Ind. Eng. Chem. Process. Des. Dev. (1985), https://doi.org/10.1021/i200031a031.

[52] Y. Lin, C. Zhang, M. Zhang, J. Zhang, Deoxygenation of bio-oil during pyrolysis of biomass in the presence of CaO in a fluidized-bed reactor, Energy Fuel (2010), https://doi.org/10.1021/ef1009605.

[53] B. Valle, N. García-Gómez, A. Remiro, J. Bilbao, A.G. Gayubo, Dual catalyst-sorbent role of dolomite in the steam reforming of raw bio-oil for producing H2-rich syngas, Fuel Process. Technol. (2020), https://doi.org/10.1016/j.fuproc.2019.106316.

[54] M. Hervy, R. Olcese, M.M. Bettahar, M. Mallet, A. Renard, L. Maldonado, D. Remy, G. Mauviel, A. Dufour, Evolution of dolomite composition and reactivity during biomass gasification, Appl. Catal. A Gen. (2019), https://doi.org/10.1016/j.apcata.2018.12.014.

[55] J. Piskorz, D.S.A.G. Radlein, D.S. Scott, S. Czernik, Pretreatment of wood and cellulose for production of sugars by fast pyrolysis, J. Anal. Appl. Pyrolysis (1989), https://doi.org/10.1016/0165-2370(89)85012-0.

[56] Q. Lu, Z.F. Zhang, C.Q. Dong, X.F. Zhu, Catalytic upgrading of biomass fast pyrolysis vapors with nano metal oxides: an analytical Py-GC/MS study, Energies (2010), https://doi.org/10.3390/en3111805.

[57] O.D. Mante, J.A. Rodriguez, S.D. Senanayake, S.P. Babu, Catalytic conversion of biomass pyrolysis vapors into hydrocarbon fuel precursors, Green Chem. (2015), https://doi.org/10.1039/c4gc02238f.

[58] J. Gupta, K. Papadikis, E.Y. Konysheva, Y. Lin, I.V. Kozhevnikov, J. Li, CaO catalyst for multi-route conversion of Oakwood biomass to value-added chemicals and fuel precursors in fast pyrolysis, Appl. Catal. B Environ. (2021), https://doi.org/10.1016/j.apcatb.2020.119858.

[59] H.V. Ly, J.W. Park, S.S. Kim, H.T. Hwang, J. Kim, H.C. Woo, Catalytic pyrolysis of bamboo in a bubbling fluidized-bed reactor with two different catalysts: HZSM-5 and red mud for upgrading bio-oil, Renew. Energy (2020), https://doi.org/10.1016/j.renene.2019.10.141.

[60] J. Wildschut, J. Arentz, C.B. Rasrendra, R.H. Venderbosch, H.J. Heeres, Catalytic hydrotreatment of fast pyrolysis oil: model studies on reaction pathways for the carbohydrate fraction, Environ. Prog. Sustain. Energy (2009), https://doi.org/10.1002/ep.10390.

[61] K. Iisa, D.J. Robichaud, M.J. Watson, J. Ten Dam, A. Dutta, C. Mukarakate, S. Kim, M.R. Nimlos, R.M. Baldwin, Improving biomass pyrolysis economics by integrating vapor and liquid phase upgrading, Green Chem. (2018), https://doi.org/10.1039/c7gc02947k.

[62] D.B. Levin, R. Chahine, Challenges for renewable hydrogen production from biomass, Int. J. Hydrog. Energy (2010), https://doi.org/10.1016/j.ijhydene.2009.08.067.